PUBLICATION V

Drilling of conventional cast stainless steel with HIPed NiTi coating

In: Journal of Materials Processing Technology 2004.
Vol. 153–154, pp. 622–629.

ELSEVIER

Journal of Materials Processing Technology 153–154 (2004) 622–629

Journal of Materials Processing Technology

www.elsevier.com/locate/jmatprotec

Drilling of conventional cast stainless steel with HIPed NiTi coating

J.A. Paro*, T.E. Gustafsson, J. Koskinen

VTT Industrial Systems, VTT Manufacturing Technology, Materials and Manufacturing Technology, P.O. Box 1703, Espoo VTT 02044, Finland

Abstract

This study investigated suitability of TiN- and TiCN-coated cemented carbide tools in the machining of conventionally produced stainless steel with hot isostatic pressed (HIPed) NiTi coating. Near-equiatomic nickel–titanium alloy (NiTi) has many attractive material properties, such as pseudo-elasticity and shape memory effects, which result into beneficial engineering properties, e.g. as cavitation resistant coatings in addition to its well-known shape memory properties. Stainless steels are often considered to be poorly machinable materials; materials with high elasticity are also difficult to machine. In drilling stainless steel with a pseudo-elastic-coating material, machinability difficulties are caused by the high strength and work hardening rate of steel and the pseudo-elastic properties of the coating material. In this study, drilling tests were carried out by a machining center. The machinability was studied by analyzing cemented carbide drills and chips. The interface between stainless steel and NiTi coating was examined with scanning electron microscopy (SEM) and energy dispersive spectroscopy (EDS) analysis. The effect of feed rate on chip formation and tool wear was analyzed. The cutting tests indicated that cutting speeds of 50 m/min, a feed rate of 0.1–0.2 mm/rev, and solid carbide drills can be applied, from a machinability standpoint. A HIPed pseudo-elastic coating decreases machinability. When effective cutting speeds and feed rates were utilized, optimal tool life was achieved without a decrease in coating properties.

Keywords: Drilling; Stainless steel; NiTi coating

1. Introduction

Austenitic stainless steels are considered to be difficult to machine. Built-up edge (BUE) and irregular wear situations are often faced in machining operations. Difficulties from the machining point of view increase when duplex and high-strength stainless steels are to be machined [1].

One important characteristic of shape memory alloys (SMAs) is their super-elastic property. The NiTi polycrystalline SMA has, due to its unique bio-compatibility and super-elasticity, been successfully used to manufacture medical devices in recent years. One of the most dramatic-appearing examples is the utility of super-elastic coatings. Near-equiatomic nickel–titanium alloys (NiTi) have many attractive properties for engineering applications, such as pseudo-elasticity and good cavitation resistivity, in addition to their more well-known shape memory properties [2,3]. Nevertheless, both technical and commercial limitations arise when NiTi is considered as a material for large engineering components. Consequently, interest in NiTi-coating technologies is on the rise.

One of the principal challenges in NiTi coating is how to achieve adequate adhesion between NiTi and the substrate material. Explosive welding has been used successfully as a NiTi-coating method [4,5]. However, due to the nature of explosive welding, the surface to be coated must not have a very complex geometry. Thermal spraying has also been investigated, but, unfortunately, thermally sprayed NiTi on steel substrates has been reported to have poor adhesion. It has been suggested that the poor adhesion is due to a thermal expansion mismatch between the coating and the substrate [5]. Fusion-welded coatings suffer from poor adhesion because of the formation of brittle inter-metallic reaction layers [6].

It is known that hot isostatic pressing (HIP) can be used to produce bulk NiTi components from powders [7–9]. In the present study, machining of NiTi-coated stainless steels has been investigated as a potential NiTi-coating method for stainless steels.

* Corresponding author. Tel.: +358-9-456-5414; fax: +358-9-463-118.
E-mail address: jukka.paro@vtt.fi (J.A. Paro).

0924-0136/$ – see front matter © 2004 Elsevier B.V. All rights reserved.
doi:10.1016/j.jmatprotec.2004.04.100

Table 1
The nominal composition (%) of the steel used in the drilling experiment

C	0.03
Mn	1.20
S	0.015
P	0.04
Cr	18.4
Ni	9.2
Si	0.4
V	0.06

2. Materials

The samples used in the drilling tests were firstly machined from the stainless steel blocks (X2CrNi 1911). The nominal composition of the test steel is presented in Table 1. The capsule (Fig. 1a) for HIP operation was welded from stainless steel plate (AISI 316) onto this block. The capsule was filled with rotating disc atomized NiTi powder (FUKUDA®) with an average particle size of 0.23 mm and composition 49.4 ± 4.7 at.% Ni and 50.6 ± 4.7 at.% Ti. The target bulk material composition (Ni/Ti) is 50/50 at.%, which is 55/45 wt.% (see Fig. 1b). After the HIPing of the NiTi powder onto the block, the capsule was removed with a solid carbide milling tool for later drilling tests.

3. Methods

The HIP treatment was used to sinter coatings from NiTi powder on the base material block. These samples were mounted in a stainless steel capsule that was evacuated to a pressure of 10^{-5} mbar. The HIPing parameters were 900 °C, 100 MPa, and 3 h. The cooling rate was 4.6 K/min.

Drilling tests were carried out using a horizontal machining center. The tests used TiCN- and TiN-coated cemented carbide drills with a diameter of ∅ 8.5 mm, at a cutting speed of 50 m/min and feed rates of 0.1, 0.15, and 0.2 mm/rev. Drilling tests were done both with and without through-spindle cooling. Pseudo-elasticity of the HIPed NiTi coating was tested with Vickers hardness measurements, using a load of 9.81 N.

From the drilled test piece, cross-sectional samples were cut out along the drill axis. These samples were polished and etched with picric acid and with NaOH–water solution with electrolytic etching.

The NiTi powder and HIPed coating cross-sections, and cross-sections of the drilling test samples, were studied in detail with an optical microscope (OM) and scanning electron microscope (SEM). The NiTi powder was collected on an electrically conductive graphite adhesive, and the powder sample on the adhesive was studied with the SEM and analyzed with an X-ray analyzer (EDS), which can detect sodium (Na) and elements heavier than that. The compositions of the particles ($N = 15$) and that of the details in the drilling test cross-sections were determined from the X-ray spectra using a correction factor program (ZAF). The X-ray lines used in the analysis were iron (Fe), chromium (Cr), manganese (Mn), nickel (Ni), titanium (Ti), and silicon (Si). To calibrate the magnification of the microscope and to perform the X-ray analysis, ASTM practices E766-98, E1508-98, when applicable were used, respectively. In SEM images obtained with a 25 kV acceleration voltage at a working distance of 20 mm, the error in the magnification is ±2%. The smallest detectable content in the X-ray analysis is approximately 0.3–0.5% for metals, depending on the composition of the material analyzed.

4. Results

The HIPed NiTi coating is shown in Fig. 2. The NiTi powder has sintered into solid material, in which only some inter-granular pores could be detected. The hardness was tested with a Vickers-hardness measuring device, from both

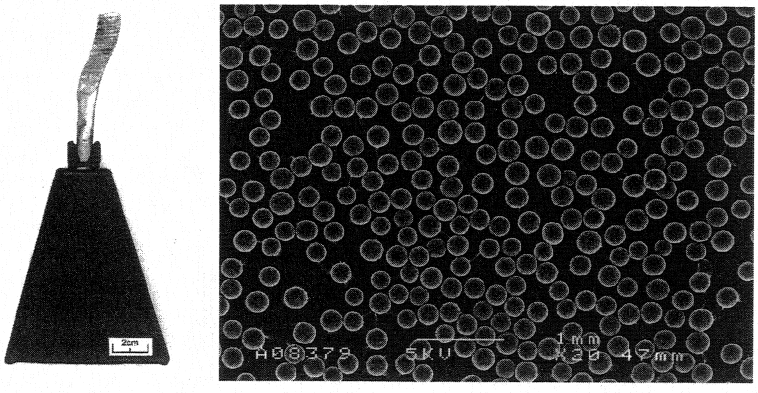

(a) (b)

Fig. 1. (a) The HIPing capsule and (b) NiTi powder used in the experiment.

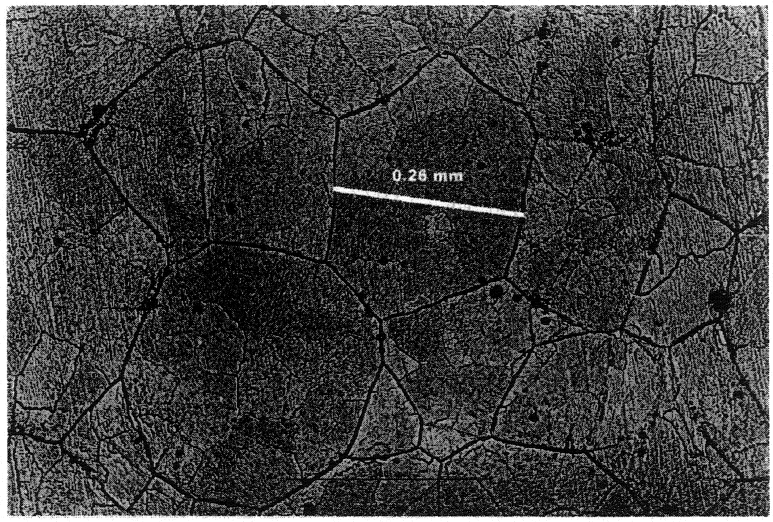

Fig. 2. NiTi coating after HIPing—magnification 200×.

the steel and the NiTi coating. The hardness print of the steel shows a typical Vickers imprint (Fig. 3a) on the steel surface, whereas the imprint on the NiTi coating shows retraction of the material on the imprint edges (Fig. 3b). The retraction is due to the pseudo-elastic nature of the NiTi coating.

The interface between the coating and the steel was studied after making longitudinal polished and etched cross-sections from the drilled hole edge and drilling chips. The interface between the coating and base material is shown in Fig. 4a and b.

The interface between the HIPed NiTi coating and the steel showed two distinct features. First, there was a layer of iron that diffused into the NiTi coating; this had a thickness of approximately 20 μm. The second feature is the layer on the steel side, which was enriched in chromium to a level of 28.4% Cr due to the diffusion of iron into the NiTi coating (Table 2, Fig. 4b). Also, titanium diffusion into the steel surface layer, a few micrometers in thickness, was observed. A more detailed study of the interface layer on the steel side showed internal structure in the layer, which seems to form more easily in the ferrite phase than in the austenite phase of the steel (Fig. 5a and b).

The results presented in Table 2, from the points in Fig. 4b, show diffusion of iron and chromium into NiTi. The diffusion of iron is stronger than that of the chromium, leading to the observed chromium enrichment at the steel-edge layer (Figs. 4b and 6, points 21–25).

The cutting edges with TiN and TiCN-coated drills that were examined by SEM analysis are shown in Fig. 7a and b. Fig. 7a shows the unused cutting edge of a solid carbide drill, and Fig. 7b shows the edge after drilling without internal through-spindle cooling and with a machining speed of 50 m/min and feed rate of 0.1 mm/rev. The same cutting edge was analyzed with SEM and EDS (Fig. 8b).

A nickel- and titanium-rich layer was found at the cutting edge between the edge and the steel chip adhering to it (Fig. 8a and b).

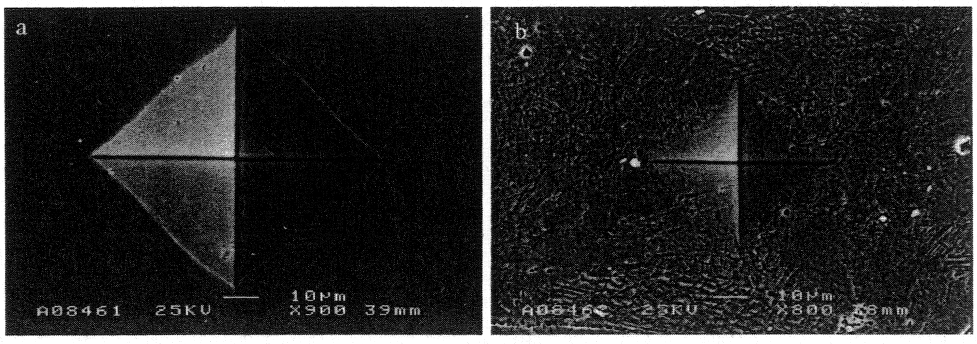

Fig. 3. SEM images of (a) the Vickers hardness indentation (HV1) in the steel and (b) Vickers hardness indentation (HV1) in the NiTi coating.

Table 2
The EDS element analysis at points presented in Fig. 4b

Analysis	Fe (%)	Cr (%)	Ni (%)	Mn (%)	Si (%)	Ti (%)
Points 1–5	1.8 ± 0.1	n.d.	49.8 ± 2.5	n.d.	n.d.	48.1 ± 2.4
Points 6–10	5.1 ± 0.1	0.4 ± 0.1	46.0 ± 0.5	n.d.	n.d.	48.4 ± 0.5
Points 11–15	8.5 ± 0.2	0.7 ± 0.1	42.4 ± 0.3	n.d.	n.d.	48.3 ± 0.4
Points 16–20	40.6 ± 2.4	7.5 ± 0.4	12.2 ± 1.0	0.4 ± 0.1	~0.3	38.9 ± 2.7
Points 21–25	51.7 ± 3.2	28.4 ± 1.9	5.1 ± 0.4	0.8 ± 0.1	~0.2	13.8 ± 5.4
Points 26–30	67.5 ± 0.2	19.3 ± 0.5	11.6 ± 0.5	~1.0	~0.3	~0.3

A change in chip morphology was detected between the NiTi coating and steel chips. First, when the NiTi coating is drilled, the chip is deformed strongly. The chips are conical and strongly spiral in form. Second, when the drill has reached the interface between the NiTi coating and stainless steel, the shape becomes that of conventional stainless steel chips. The chips encountered during the drilling operation were also red-hot. These chips, produced at a cutting speed of 50 m/min and feed rate of 0.1 mm/rev, are shown in Fig. 9a.

In Fig. 9b is presented a stainless steel and NiTi chip boundary. A detailed image of the interface (Fig. 10a) shows good adhesion between the materials, even when the NiTi's pseudo-elasticity has been exceeded during the drilling (Fig. 10b).

Fig. 11a and b shows the influence of feed rate on the NiTi coating's structure after drilling. In Fig. 11b, a cutting speed of 50 m/min and feed rate of 0.1 mm/rev were used, whereas for Fig. 10a the feed rate was increased to 0.3 mm/rev. Cutting fluid through spindle during these drilling operations was not applied. Fig. 11b also shows the points for EDS analyses, with results listed in Table 3. No apparent diffusion of steel or NiTi elements over the adhered interface was found. The NiTi grains nearest to the drill hole showed a size increase on account of heat. This was not found in the bulk material.

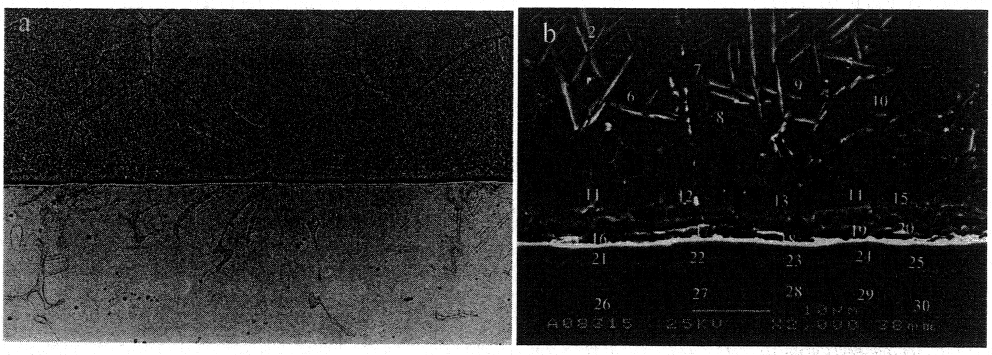

Fig. 4. (a) Optical micrograph of the NiTi coating and stainless steel interface and (b) an SEM image of the interface with points used for quantitative EDS element analysis. Etched with picric acid.

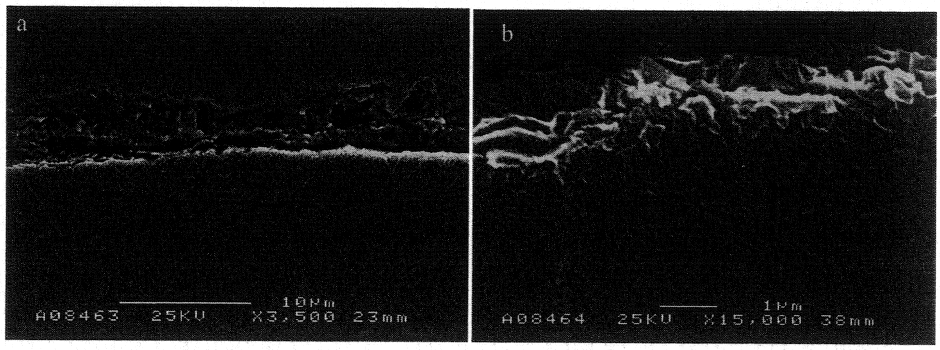

Fig. 5. (a) The NiTi coating and steel interface after electrolytic etching in NaOH–water solution and (b) a detail from the interface on the steel side in the layer with analysis points 21–25 in Fig. 4b.

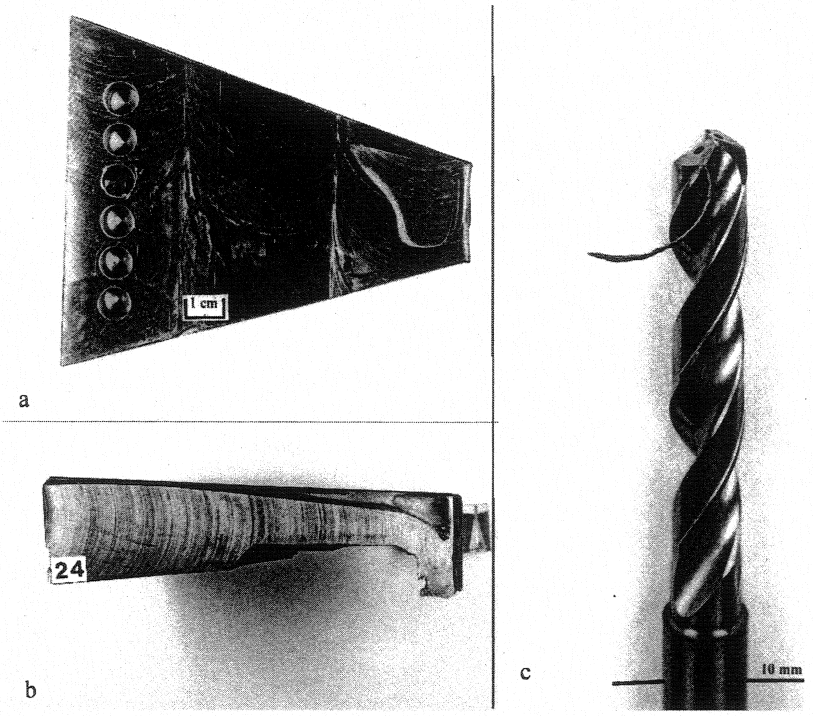

Fig. 6. (a, b) The workpiece of stainless steel with NiTi coating used in drilling tests and (c) a TiN-coated ∅ 8.5 mm solid carbide drill used in drilling tests showing chip buildup on the cutting edge.

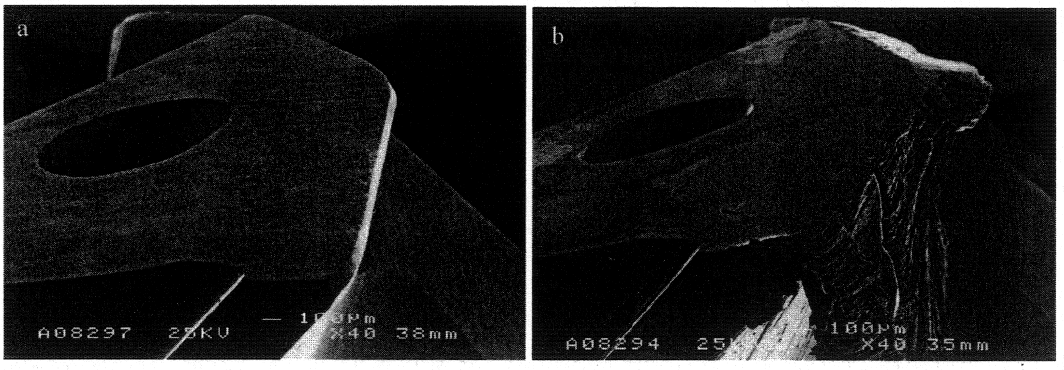

Fig. 7. (a) SEM image of an unused TiCN- and TiN-coated solid carbide drill's cutting edge and (b) the built-up edge (BUE).

With optimum machining parameters, some expiration of the grain boundaries of NiTi was detected (Fig. 12a and b). This sample was produced at a cutting speed of 50 m/min and feed rate of 0.1 mm/rev by applying coolant through the spindle. In comparing Figs. 11b and 12a, the effect of cooling can be seen in decreased steel buildup on the NiTi. Also, the surface topography was found to be much smoother than with inferior cooling properties or higher feed rates.

5. Discussion

The stainless steel workpiece with NiTi coating was produced by HIP treatment, and sufficient adhesion properties were achieved. After a machining operation was performed on the capsule, the interface between the stainless steel block and NiTi coating was intact. The drilling experiments showed that the tool wear mechanism for NiTi-coated stainless steel was similar to that with conventional stainless steel.

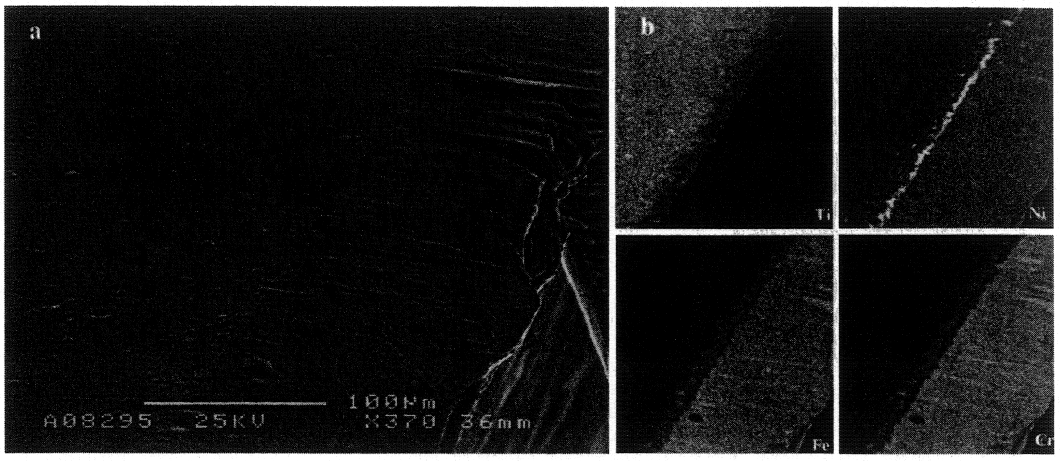

Fig. 8. (a) The cutting edge of a solid carbide drill with BUE and (b) EDS analyses showing the distribution of Ti, Ni, Fe, and Cr within the field of view.

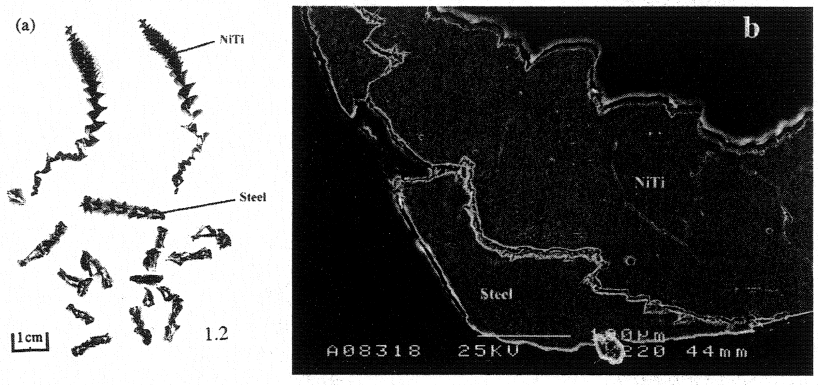

Fig. 9. (a) Chips from drilling of NiTi-coated stainless steel and (b) an SEM image of the deformation of the interface between the steel and NiTi coating.

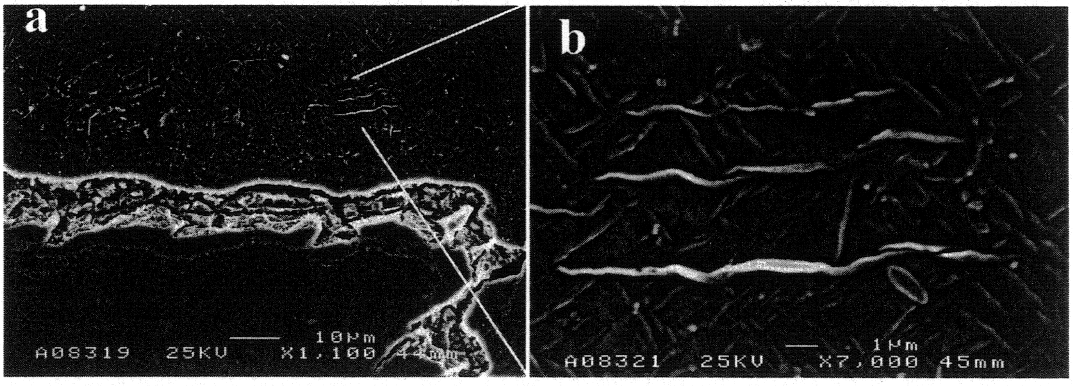

Fig. 10. (a) A detail from Fig. 9b, showing deformation of the stainless steel and NiTi interface in the chip and (b) a detail of the deformed NiTi coating detected in the chip when the load had exceeded the pseudo-elasticity of NiTi during drilling.

Table 3
Point analyses of drilled NiTi hole with stainless steel buildup layer (Fig. 11b)

Analysis	Fe (%)	Cr (%)	Ni (%)	Mn (%)	Si (%)	Cu (%)	Ti (%)
Points 1–5	68.2 ± 0.2	19.8 ± 0.5	10.6 ± 0.5	~0.9	~0.3		
Points 6–10	0.8 ± 0.3	0.2	55.1 ± 0.2			~0.2	43.7 ± 0.2
Points 11–15			55.1 ± 0.3				44.7 ± 0.3

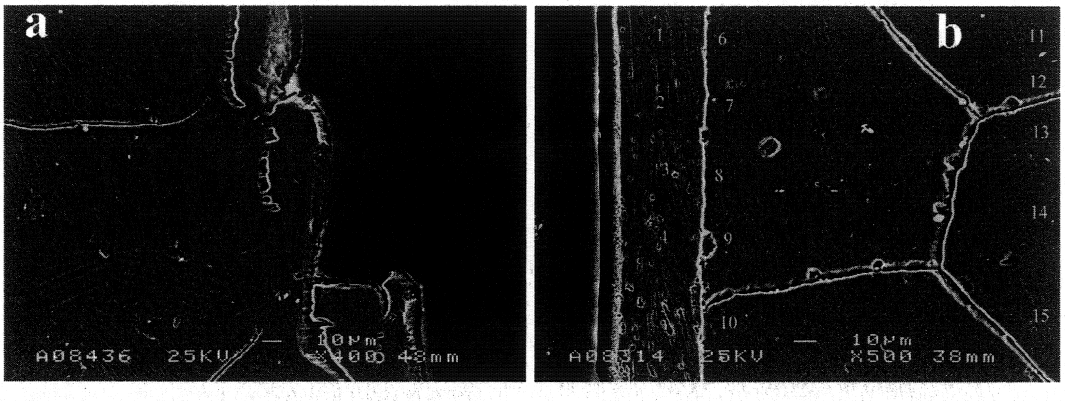

Fig. 11. SEM images of holes drilled in the NiTi coating: (a) cutting speed of 50 m/min and feed rate of 0.2 mm/rev, showing rough surface structure; (b) 0.1 mm/rev, showing steel buildup on the drilled hole wall.

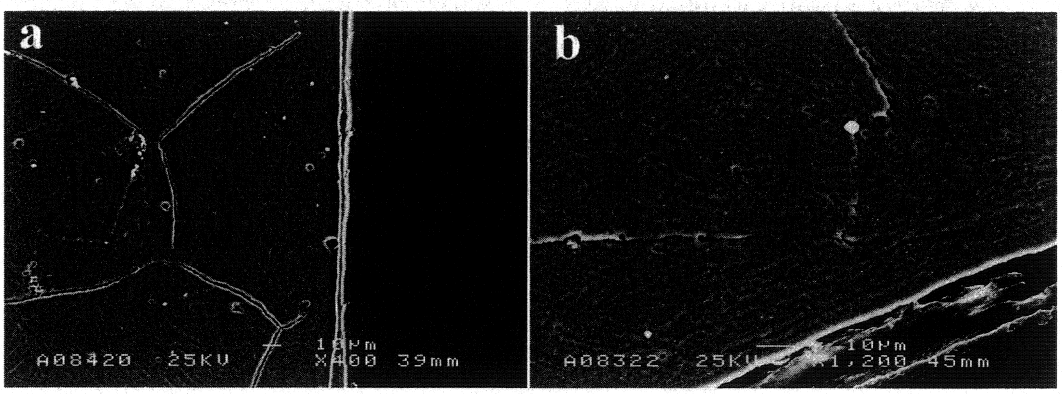

Fig. 12. SEM images of drilled NiTi coating with optimum cutting speed of 50 m/min and feed rate of 0.1 mm/rev, with cutting fluid applied through the spindle.

The interface between steel and the NiTi coating was studied via SEM and EDS analyses. For future investigation of the microstructure of the interface between stainless steel and NiTi coating, transmission electron microscopy (TEM) should be carried out to map out the microstructure in heat-affected diffusion layers originating from the HIPing process.

The first drilling showed strongly deformed chips which have been red-hot. Their deformation may be related to shape memory effects. The opening chips also showed good adhesion between NiTi and stainless steel, as these chips were found to be unbroken. The formation of the BUE detected in drills might have been enhanced by the tool coating (TiCN and TiN), which in turn also merits further investigation.

When sensitive feed rate values are used, the drilled hole wall remains smooth, with only a small amount of steel stuck to the NiTi. Increasing the feed rate causes the surface topography to be roughened. Using internal cooling through the spindle in solid carbide drills makes the hole surface topography even smoother.

The NiTi diffusion layers were found to be affected by the heat from HIPing, and the NiTi grain boundaries affected by the strong plastic deformation during drilling operations in the vicinity of the hole wall.

6. Conclusions

From the results obtained in the study, the following conclusions were drawn. The drilling of NiTi-coated stainless steel with sufficient cutting parameters is possible without severe tool wear. A cutting speed of 50 m/min and feed rate between 0.1 and 0.2 mm/rev with solid carbide drills and through-spindle cooling should be applied. Tool wear mechanisms in through-spindle cooling are similar to those encountered with stainless steel.

The macroscopic geometry of stainless steel chips with NiTi coating differs from conventional stainless steel chips. The opening chips are constructed from the NiTi concatenated with conventional long stainless steel chips, and the adhesion in the interface layer between NiTi coating and stainless steel remains intact in the chip formation process.

There are stainless steel residues on NiTi drilled hole walls. An increased supply of cutting fluid has an advantageous effect on the surface properties of the hole. The amount of stainless steel adhering to the NiTi walls is decreased when cutting fluid is injected through the spindle. An increase in feed rate will decrease the surface quality of the drilled hole.

Strongly deformed layer on the drilled surface of NiTi was observed been deformed in excess of the pseudo-elasticity.

There is a diffusion layer of iron in the NiTi coating, and there is also a layer extending inward on the steel side, which has been enriched in chromium due to the HIP process.

Acknowledgements

The authors are thankful to Sulzer Pumps, Finland, for providing the tested stainless steel materials.

References

[1] L. Jiang, H. Hänninen, J. Paro, V. Kauppinen, Active wear and failure mechanisms of tin-coated high speed steel and tin-coated cemented carbide tools when machining powder metallurgically made stainless steels, Metall. Mater. Trans. A 27 (9) (1996) 2796–2808.

[2] Z. Li, Q. Sun, Growth of macroscopic martensite band in nano-grained NiTi microtube under tension, Int. J. Plast. 18 (2002) 1481–1498.

[3] D. Starosvetsky, I. Gotman, TiN coating improves the corrosion behaviour of superelastic NiTi surgical alloy, Surf. Coat. Technol. 148 (2001) 268–276.

[4] C. Zimmerly, T. Inal, R. Richman, Explosive welding of a near-equiatomic nickel–titanium alloy to low-carbon steel, Mater. Sci. Eng. A 188 (1994) 251–254.

[5] R. Richman, A. Rao, D. Kung, Cavitation erosion of NiTi explosively welded to steel, Wear 181–183 (1995) 80–85.

[6] P. Jardine, Y. Field, H. Herman, D. Marantz, K. Kowalsky, Processing and properties of arc-sprayed shape memory effect NiTi, Scripta Met. Mater. 24 (1990) 2391–2396.

[7] G. Wang, Welding of nitinol to stainless steel, in: Proceedings of the SMST-97, 1997, pp. 131–136.

[8] J. Koskinen, E. Haimi, A. Mahiout, V. Lindroos, S.-P. Hannula, Superelastic NiTi coatings with good corrosive wear resistance, in: Proceedings of the International Conference on Martensitic Transformations (ICOMAT'02), Espoo, 2002, pp. 10–14.

[9] J. Koskinen, E. Haimi, Method for forming a nickel–titanium plating, US Patent 6,458,317 (2002).